DOI: https://doi.org/10.57233/ihcfs.048

ISBN: 978-978-68-07775

BOOK OF PROCEEDINGS

IHCFS – 2025 WEBSITE: fos.fugusau.edu.ng

1ST INTERNATIONAL HYBRID CONFERENCE OF FACULTY OF SCIENCE

(A PUBLICATION OF FACULTY OF SCIENCE, FEDERAL UNIVERSITY GUSAU, NIGERIA)

Variable Pressure and Injection Effects on Jeffery Fluid Flow in a Porous Medium with Velocity Slip Boundary Condition

Naziru Saad[a,b], Emmanuel Omokhuale[b], Laminu Idris[b] and Samaila Musa[c]

[a]Department of Mathematics, Zamfara State University Talata Mafara, Nigeria.

[b]Department of Mathematical Sciences, Federal University Gusau, Zamfara State, Nigeria.

[c]Department of Computer Science, Federal University Gusau, Zamfara State, Nigeria.

Corresponding Author's Email: nazykaura01@gmail.com

ABSTRACT

Fluids composed of Jeffrey are collectively known as non-Newtonian fluids. Some of the application areas include: electronic cooling, and designing along with optimizing of Magnetohydrodynamic pump and generator coupled with their heat transfer in different industrial processes. The aim of the present study is to investigate variable pressure and injection on Jeffery fluid flow in a porous medium velocity slip boundary condition. It deals with an electrically conducting fluid that is incompressible and has a uniform magnetic field that is applied perpendicular to the flow. The proposed physical context is represented by the partial differential equations covering boundary conditions. To solve the boundary value problem, the system of nonlinear equations is reduced to ordinary differential equations and solved analytically using the regular perturbation technique. The graphical representations of velocity, temperature and concentration profiles are provided to illustrate their variations in response to changes in several parameters. The results of the study indicate that, the momentum boundary layer rises as the values of heat absorption and Jeffery parameters are increased, while higher values of the suction and chemical reaction parameter suppress the velocity of the fluid. Also, the temperature of the fluid becomes lower as heat generation is significant, and a reverse trend is seen when suction is increased. Increase in heat absorption parameter causes an increase in the concentration of the fluid. The outcomes of this study are applicable to magnetically controlled thermal systems, non-Newtonian polymer processing, biomedical transport modeling, and high-performance electronic cooling, where precise control of flow, heat and mass transfer is critical.

Keywords: Variable pressure, injection, Jeffery fluid, porous medium, and velocity slip.

NOMENCLATURE AND GREEK LETTERS

Nomenclature

T'	Temperature of fluid (K)
T'_w	Temperature of fluid near to moving plate (K)
T'_∞	Temperature of fluid near to stationary plate (K)
C'	Concentration of fluid (mol m^{-3})
C'_w	Concentration of fluid near to moving plate (mol m^{-3})
C'_∞	Concentration of fluid near to the stationary plate (mol m^{-3})
t'	Time in $x'and\ y'$coordinate system (s)
t	Time in dimensionless coordinates (s)
U	Reference velocity (ms^{-1})
k'	Mean absorption coefficient
g	Acceleration due to gravity (ms^{-1})
Q_0	The heat generation constant
V_0	velocity vector field
B_o	magnetics flux density (kgm^1)
B_T	plastic dynamic viscosity of non-Newtonian fluid

DOI: https://doi.org/10.57233/ihcfs.048

ISBN: 978-978-68-07775

BOOK OF PROCEEDINGS

IHCFS – 2025 WEBSITE: fos.fugusau.edu.ng

U' Dynamic viscosity of base fluid
y' Dimensional coordinate perpendicular to the plate
U_0 Dimensional velocity of the fluid
V' Fluid velocity (nondimensional) (ms^{-1})
y Dimensional coordinate perpendicular to the plate
G_l Mass diffusion coefficient
G_r Thermal Grashof number
Kc Chemical reaction parameter
M Magnetic parameter
R Thermal radiation parameter
S Suction parameter
Sc Schmidt number

Greek Letters

β Deborah number
γ Jeffery parameter
ϵ Amplitude of modulation
δ Boundary layer thickness
$\emptyset$ Nanoparticle volume fraction
λ Retardation time
ξ Dimensional coordinate perpendicular to the plate
υ Kinematic viscosity
σ Density
η Fractional parameter

1.0 INTRODUCTION

The Jeffery fluid is a specific type of matter which easily goes under deformation when an external force is applied, and it has no particular shape. Mainly, fluids are partitioned as Newtonian fluid and non-Newtonian fluids. Non-Newtonian fluids have numerous practical and industrial applications, and such fluids involve honey, blood, greases, oils, and food stuff (Anwar *et al.,* 2021). The boundary layer problems are given more consideration nowadays, this may not be unconnected with roles it plays in the areas of technology, engineering and industrial applications. Radiation effects on heat and mass transfer are of greater importance in many processes and have, therefore, received a considerable amount of attention in recent time, for example nuclear reactor, solid matrix heat exchanger, thermal insulation, surface catalysis of chemical contaminants in various processes, storage of nuclear waste materials, grain storage and drying and many others (Ahmad & Sarki, 2023). Porous medium has garnered significant attention in heat transfer, and it removes heat from reactors, heat exchangers, solar energy, etc. Over the past two decades, numerous researchers have dedicated their efforts to studying heat transfer phenomena specifically within porous media. A porous medium is a substance that contains pores, or spaces between solid materials through which liquid or gas can pass. Omowaye *et al.* (2015) presented an analytical method of solution to steady two-dimensional hydromagnetic flow of a viscous incompressible, electrically conducting fluid past a semi-infinite moving permeable plate embedded in a porous medium. It is assumed that the fluid properties are constant except for the fluid viscosity which vary as an inverse linear function of temperature. The boundary layer equations were transformed in to a coupled ordinary differential equation with the help of similarity transformations. They solved the resulting coupled ordinary differential

DOI: https://doi.org/10.57233/ihcfs.048

ISBN: 978-978-68-07775

BOOK OF PROCEEDINGS

equations were solved using the Homotopy Analysis Method (HAM). The influence of Joule heating and induced magnetic field on magnetohydrodynamics generalised Couette flow of Jeffrey fluid in an inclined channel through a porous medium.

It is applied in engineering fields and physiology such as transpiration, cooling gaseous diffusion and blood flow in arteries. The flow through the porous media occurs on the ground water hydrology. Irrigation and drainage problems are critical areas of greater concern, henceforth, scientific treatment of the problems of irrigation, soil erosion and tile drainage are some of the recent developments of porous media. Several researches indicated significant effects of slip condition on many problems of physical interest, among which are boundary layer flow control, plasma studies, geothermal energy extraction, metallurgy, chemical, mineral and petroleum engineering to mention but few (Ahmad & Sarki, 2023). Additionally, studying heat and chemical reactions in fluid flows contributes to understanding pollutant dispersion from industrial sources and improving combustion efficiency to reduce emissions (Krishna & Reddy, 2025).

Gulle and Kodi (2022) undertook research on a study of the unsteady magneto-hydrodynamic mixed convection Jeffery fluid flow over an inclined permeable moving plate in the presence of thermal radiation, heat generation, radiation, aligned magnetic field, thermophoresis effect and homogeneous chemical reaction subjected to variable suction analytically. Effects of heat and mass transfer of MHD Jeffery nanofluid flow with chemical reaction, radiation and soret was investigated by (Haritha *et al.*, 2022). Raghunath *et al.* (2022) examined unsteady MHD flow of a Jeffery fluid through a porous medium in the presence of heat absorption and chemical reaction.

On the other hand, radiative convective flows are encountered in countless industrial and environmental processes, particularly in astrophysical studies and space technology. Radiative heat and mass transfer play an important role in manufacturing industries for the design of fins, steel rolling, nuclear power plants, gas turbines and various propulsion device for aircraft, combustion and furnace design, materials processing, energy utilization temperature measurements, remote sensing for astronomy and space exploration, food processing cryogenic engineering as well as numerous agricultural health and military applications.

Sharma *et al.* (2022) presented the numerical study of MHD oscillatory flow of viscous dissipative fluid along an upstanding channel entrenched with porous medium due to heat source and thermal radiation impacts. The study of thermal radiation effect, which is the electromagnetic wave radiation that a surface generates because of its heat, is gaining growing attention, especially when a magnetic field is applied, due to its relevance in constructing different advanced energy conversion systems capable of operating at high temperatures (Jamaludin *et al.* 2020). Other areas of possible advantages include nuclear plants, solar technology, spacecraft aerodynamics, to state a few. In view of this, several scholars have carried out investigations on the impact of heat radiation in a number of physical configurations. With the numerous advantages of thermal radiation in mind, Hamza *et al.* (2023) recently scrutinized the consequences of thermal radiation and super-hydrophobicity on a magnetized natural convection fluid through a heated porous superhydrophobic microchannel. Shah *et al.* (2023) investigated the impact of heat transfer in MHD Casson flow in the presence of thermal and chemical reactions influenced by thermal fluid properties. Ojemeri *et al*. (2023) put forth MHD flow of an electrically conductive Casson fluid with thermal radiation effect in a vertical porous plate, Using Darcy's model, Gireesha *et al.* (2020) outlined how thermal radiation and free convection affected the flow of a water-based hybrid nanofluid containing nanoparticles through a porous vertical channel, and Goud *et al.* (2023)

DOI: https://doi.org/10.57233/ihcfs.048

ISBN: 978-978-68-07775

BOOK OF PROCEEDINGS

examined the analysis of transient MHD flow through a permeable medium across an upright plate in the context of the coexistence of viscous dissipation and thermal radiation effects. Omokhuale and Dange (2023a) extended this phenomenon to reveal the impact of heat absorption on unsteady MHD convective Jeffery flow of a viscous, electrically conducting and incompressible fluid. Furthermore, Omokhuale and Dange (2023b) focused on extending their research to investigate chemical reaction and radiation absorption effects on MHD Jeffery fluid. Recently, Naz and Tamizharasi (2025) presented a rheological model for magnetohydrodynamic Jeffrey fluid flow past an inclined permeable vertical surface under the influence of injection/suction, mixed convection and a decaying pressure gradient.

In this paper, variable pressure and injection effects on Jeffery fluid flow in a porous medium with velocity slip boundary condition has been investigated. The governing equations are solved using regular perturbation method. The expressions for the skin-friction, rate of heat and mass transfer were deduced from the solutions of velocity, temperature and concentration obtained. The effects of physical parameters of engineering interest on velocity, temperature and concentration solutions analysed and presented graphically.

2.0 MATHEMATICAL FORMULATION

Consider the flow of incompressible Jeffery fluid in a vertical plate with saturated porous medium chosen along the plate under the influence of an externally applied homogeneous magnetic field. A magnetic field of uniform strength B_0 is applied transversely to the plate. The flow is further assumed to be in the $x'-$ axis direction which is taken to be vertically upward along the channel walls and $y'-$ axis is taken to be normal to the plate that are ∞ distance apart. Initially, the plate and the fluid are at same temperature T' with concentration level C' at time $t'>0$, the plate and the mass concentration are raised to T'_w and C'_w causing the presence of temperature and concentration difference to be $T'-T'_\infty$ and $C'-C'_\infty$, respectively. The effects of variable pressure, injection and velocity slip are considered. Following Omokhuale and Dange (2023), The study of heat generation or absorption on fluid flow is extremely fundamental in several technological and physical problems of exothermic or endothermic fluid response nowadays, and these effects are crucial in monitoring the heat transference (Gambo *et al*., 2021). Several scholars have investigated the effects of heat-generating/absorbing fluid on various flow regimes. and under the usual Boussinesq's approximation, the governing equations in dimensional form are continuity, momentum, energy and mass equations which are as follows:

$$\frac{\partial v}{\partial y}=0 \tag{1}$$

$$\frac{\partial U'}{\partial t^I}+v'\frac{\partial U'}{\partial y^I}=\frac{\upsilon}{I+\lambda}\frac{\partial^2 U'}{\partial y^{1^2}}+g\beta_T\left(T'-T'_\infty\right)+g\beta_C(c'-C'_\infty)-\nu\frac{U'}{K'}-\frac{\sigma B_0^2}{\rho}U'+\frac{1}{P}\frac{\partial P}{\partial \varkappa} \tag{2}$$

$$\frac{\partial C'}{\partial t^I}+v'\frac{\partial C'}{\partial y^I}=D_m\frac{\partial^2 C'}{\partial y^{1^2}}-R'_c(C'-C'_\infty) \tag{3}$$

$$\frac{\partial T'}{\partial t^I}+v_o\frac{\partial T'}{\partial y^I}=\frac{K_o}{\rho cp}\frac{\partial^2 T'}{\partial y^{I2}}-\frac{Q_T}{\rho cp}\left(T'-T'_\infty\right) \tag{4}$$

Subject to the boundary conditions:

$$t'\le 0: u'=0, T'=T'_\infty, C'=C'_\infty \text{ for all } y'$$

$$t'>0\begin{cases}u'=u_p, T'=T'_\infty+(T'_w-T'_\infty)\epsilon e^{iwt}, C'=C'_\infty+(C'_w-C'_\infty)\epsilon e^{iwt} \text{ at } y'=0\\ u'\to 0, T'\to T'^I_\infty, C'\to C'^I_\infty \quad as\ y'\to\infty\end{cases} \tag{5}$$

where $\frac{1}{P}\frac{\partial P}{\partial \varkappa}=\lambda\epsilon e^{int}$ and $v'=-v_0(1+\epsilon e^{int})$

DOI: https://doi.org/10.57233/ihcfs.048

ISBN: 978-978-68-07775

BOOK OF PROCEEDINGS

Here, $v' = + v_0$ (6)

We define the following dimensionless quantities:

$$y = \frac{y^1 U_o}{\nu}, t = \frac{t^1 U_o^2}{\upsilon}, U = \frac{u^l}{u_o}, \theta = \frac{T^l - T_\infty^l}{T_w^l - T_\infty^l}, \xi = \frac{C^l - C_\infty^l}{C_w^l - C_\infty^l} \quad (7)$$

Substituting (6) and (7) into equations (2), (3) and (4), then, we have the following non – dimensional form of these equations as follows:

$$\frac{\partial u}{\partial t} - \eta \frac{\partial u}{\partial y} = \frac{I}{I+\lambda} \frac{\partial^2 U}{\partial y^2} + G_C \xi + G_r \theta - \frac{I}{K} u - Mu + \lambda \epsilon e^{int} \quad (8)$$

$$\frac{\partial \theta}{\partial t} - \eta(1 + \epsilon e^{int}) \frac{\partial \theta}{\partial y} = \frac{I}{Pr} \frac{\partial^2 \theta}{\partial y^2} + \varphi\theta + \psi\xi \quad (9)$$

$$\frac{\partial \xi}{\partial t} - \eta(1 + \epsilon e^{int}) \frac{\partial \xi}{\partial y} = \frac{I}{Sc} \frac{\partial^2 \xi}{\partial y^2} - R\xi \quad (10)$$

The corresponding initial and boundary conditions (5) in non-dimensional form become:

$U_0 = U_1 = $Up, $\xi_0 = \xi_1 = 1$, $\theta_0 = \theta_1 = 1$ at y=0

$U_0 = U_1 \Rightarrow 0$, $\xi_0 = \xi_1 \Rightarrow 0$, $\theta_0 = \theta_1 \Rightarrow 0$, at y=0

where $\tau = \frac{V_0}{U_0}$, $S_c = \frac{\upsilon'}{D}$ R= $\frac{R_c'}{U_0^2}$, $\frac{1}{pr} = \frac{\mu_{cp}}{k_T}$, $\varphi = \frac{\theta_T \nu}{\rho_{cp}\, u_0^2}$, $\psi = \frac{\theta_c \upsilon \xi\, (C_w' - C_\infty')}{(T_w' - T_\infty')u_o^2}$ $G_c = \frac{GB_1\,(T_w' - T_\infty')\nu}{U_0^2}$,

$G_r = \frac{GB_2\,(C_w' - C_\infty')\nu}{U_0^2}$. M= $\frac{\delta\beta_0^2}{U_0^2}$, K= $\frac{K'\,U_0}{\nu^2}$,

3.0 ANALYTICAL SOLUTIONS

To solve (8) to (10) subject to the boundary conditions (11), we assume approximate solutions of the form:

$$u(y,t) = u_o\,(y) + u_1(y)\epsilon e^{int} \quad (12)$$

$$\xi(y,t) = \xi_o(y) + \xi_1(y)\epsilon e^{int} \quad (13)$$

$$\theta(y,t) = \theta_o(y) + \theta_1(y)\epsilon e^{int} \quad (14)$$

Substituting (12) to (14) into (8) to (11), we have

The following are set of ODEs:

$$\theta_o : \theta_o'' + \eta pr\theta_o' + \varphi pr\theta_o = -\psi pr\xi_o \quad (15)$$

$$\theta_1 : \phi_1'' + \eta pr\theta_1' + (\varphi - in)pr\,\theta_1 = -\eta pr\theta_0' - \psi pr\xi_1 \quad (16)$$

$$\xi_o : \xi_o'' + \eta sc\,\xi_o' - Rsc\xi_o = 0 \quad (17)$$

$$\xi_1 : \xi_1'' + \eta sc\,\xi_1' - (R + in)pr\xi_I = -\eta\xi_o' \quad (18)$$

$$u_o : \frac{1}{1+\lambda}\,u_0'' + \eta\,u_0' - (\mathrm{M} + \frac{1}{K})\,u_0 = -G_c\,\xi_0 - G_r\theta_0 \quad (19)$$

$$u_1 : \frac{1}{1+\lambda}\,u_0'' + \eta\,u_1' - \left(M + \frac{1}{K} + in\right)u_1 = -G_c\xi_1 - G_r\theta_1 - \eta\;u_o' + \lambda \quad (20)$$

The corresponding boundary conditions are:

$u_o - \varphi u_0' = 0$, $u_o = \varphi u_0'$, $\theta_0 = 1$, $\theta_1 = 1$, $\xi_0 = 1$, $\xi_1 = 1$ at y=0

$u_0 = u_1 = 0$ $\theta_0 = \theta_1 = 0$ $\xi_0 = \xi_1 = 0$ as $y \to \infty$ (21)

Solving equations (16) to (20) subject to the following boundary condition (21), gives:

The approximate solutions of velocity, temperature and concentration are expressed in the following form:

$$u(y,t) = A_{16}\,e^{-n_{10}y} + A_{17}\,e^{-n_2 y} + A_{18}\,e^{-n_6 y} + A_{19}\,e^{-n_2 y} + (A_{20}\,e^{-n_{11}y} + A_{21}\,e^{-n_{12}y} + A_{22}\,e^{-n_4 y} + A_{23}\,e^{-n_2 y} + A_{24}\,e^{-n_8 y} + A_{25}\,e^{-n_2 y} + A_{26}\,e^{-n_2 y} + A_{27}\,e^{-n_4 y} + A_{28}\,e^{-n_2 y} + A_{29}\,e^{-n_9 y} + A_{30}\,e^{-n_{10} y} + A_{31}\,e^{-n_7 y} + A_{32}\,e^{-n_2 y} + A_{33}\,e^{-n_6 y} +)\,\varepsilon e^{int}$$

$$\theta(y,t) = A_7\,e^{-n_6 y} + A_8\,e^{-n_2 y} + (A_{10}\,e^{-n_8 y} + A_{11}\,e^{-n_2 y} + A_{12}\,e^{-n_2 y} + A_{13}\,e^{-n_4 y} + A_{14}\,e^{-n_2 y} +)\,\varepsilon e^{int} \quad (22)$$

$$\xi(y,t) = e^{-n_2 y} + (A_4 e^{-n_4 y} + A_5 e^{-n_2 y})\,\varepsilon e^{int} \quad (23)$$

The Skin-friction, Nusselt and Sherwood numbers respectively at surface are as follows:

DOI: https://doi.org/10.57233/ihcfs.048

ISBN: 978-978-68-07775

BOOK OF PROCEEDINGS

IHCFS – 2025 WEBSITE: fos.fugusau.edu.ng

$$C_f = -\left(\frac{dU}{dt}\right)_{t=0} = n_{10}A_{16} - n_1A_{17} + n_6A_{18} - n_2A_{19} + (n_{11}A_{20} - n_{12}A_{21} + n_4A_{22}n_8A_{23} + n_8A_{24} - n_2A_{25} + -n_2A_{26} + -n_4A_{27} + -n_2A_{28} + -n_9A_{29} + -n_{10}A_{30} + -n_7A_{31} + -n_2A_{32} + -n_6A_{33})\,\varepsilon e^{int} \quad (24)$$

$$Nu = -\left(\frac{d\theta}{dt}\right)_{t=0} = n_6A_7 - n_2A_8 - (n_8A_{10} - n_2A_{11} + n_2A_{12} - n_4A_{13} + n_2A_{14})\varepsilon e^{int} \quad (25)$$

$$Sh = -\left(\frac{d\xi}{dt}\right)_{t=0} = -n_2 - (n_4A_4 + n_2A_5)\varepsilon e^{int} \quad (26)$$

4.0 RESULT AND DISCUSSION

The velocity slip effect on variable pressure and injection effects on Jeffery fluid flow in a porous medium with velocity slip boundary condition has been formulated and solved analytically. The regular perturbation method was used to solve the governing equations of the flow field analytically. To have physical understanding of the problem, the velocity, temperature and concentration fields, numerical values have been assigned to the parameters of the flow.

4.1 Velocity Profiles

Figures 1 and 2 display the velocity profiles for different thermal Grashof number (Gc) and Mass Grashof number (Gr). The Grashof number for heat transfer signifies the relative effect of the thermal buoyancy force to the viscous hydrodynamic force in the boundary layer. As expected, it is observed that there is an enhancement in the velocity due to the rising of thermal buoyancy force. Also, as Gc increases, the peak values of the velocity increases rapidly near the porous plate and then decays smoothly to the free stream velocity. The modified Grashof number defines the ratio of the species buoyancy force to the viscous hydrodynamic force. As expected, the fluid velocity increases and the peak value is more distinctive due to increase in the species buoyancy force. The velocity distribution attains a distinctive maximum value in the vicinity of the plate and then decreases properly to approach the free stream value. It is noticed that the velocity increases with increasing values of the Grashof number for mass transfer. In the case of different values of Magnetic parameter, the profiles of the velocity of the boundary layer is presented in Figure 3. The velocity decreases with an increase in the Hartmann number. It is because that the application of transverse magnetic field will result a resistive type force (Lorentz force) similar to drag force which tends to resist the fluid flow and thus reducing its velocity. Also, the boundary layer thickness decreases with an increase in the Hartmann number. Figure 4 presents the velocity profile for different values of Permeability parameter (K). It is found that as K rises the velocity of the fluid decreases. In the boundary layer, the velocity starts by increasing to a maximum, and slowly decreases. Physically, Permeability parameter indicates thermal buoyancy characteristic of a fluid flow. The greater it gets, the more the buoyant force brought about by the temperature gradient acts upon the fluid, thereby increasing its velocity rate in the vicinity of the heated surface. The peak velocity occurs in the boundary layer where the forces of buoyancy prevail over that of viscosity. Figure 5 depicts the velocity profiles for different values of heat absorption parameter (η). The momentum boundary layer decreases when the intensity of the heat absorption increases. The effect of slip parameter (ψ) on the velocity profile is graphically presented in Figure 6. The velocity increases as the velocity slip effect becomes significant. Figure 7 illustrates the effect of injection parameter (R) on the velocity profiles. It is observed that the velocity decreases as R becomes significant. The effect of heat absorption parameter (ϕ) on

DOI: https://doi.org/10.57233/ihcfs.048

ISBN: 978-978-68-07775

BOOK OF PROCEEDINGS

the velocity profile is presented in Figure 8. It is evident that the momentum boundary layer becomes higher as (ϕ) is decreased. The velocity profiles of Figure 9 demonstrate the velocity profiles for different values of mass absorption parameter (Pr). It is found that the velocity rises with increase in δ. Figure 10 displays the velocity profiles for different values of (S_c). It is noticed that the velocity increases as s_c rises. In Figure 11, the effect of Prandtl number on the velocity profiles is shown. It is clear that the velocity boundary layer increases when the Prandtl number is increased. Figure 12 connotes the velocity profile for varied values of Jeffery parameter $(\lambda 1)$. It is seen that higher value of Jeffery parameter leads to rise in the velocity of the fluid. Figure 13 shows the effect of velocity slip on the velocity of the fluid. It is evident that higher values of the velocity heat generation constant cause a rise in the fluid velocity $(\lambda 2)$.

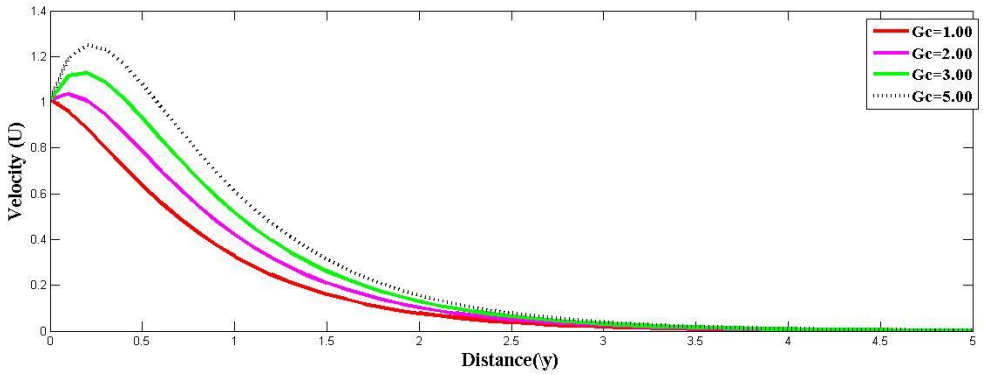

Figure 1: Velocity profile for different values of Gc.

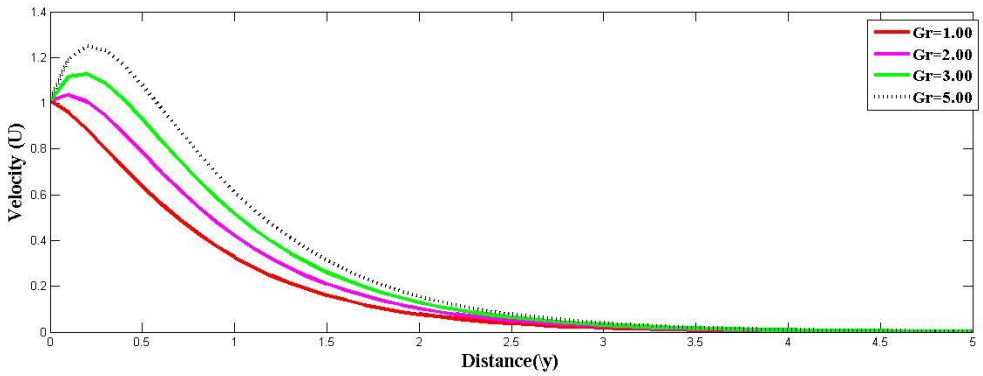

Figure 2: Velocity profile for different values of Gr.

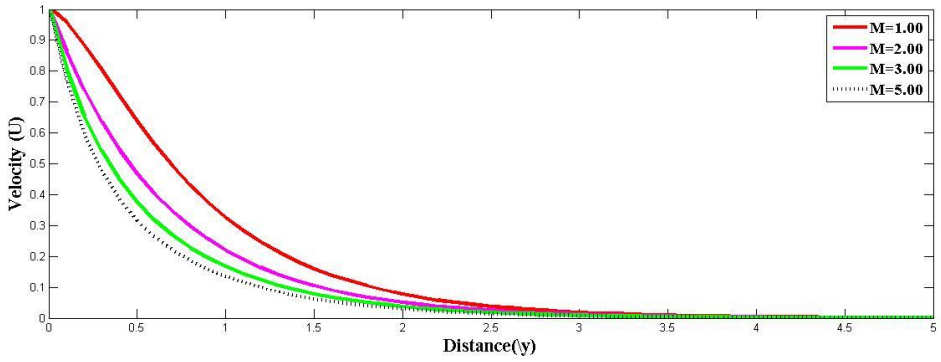

Figure 3: Velocity profile for different values of M.

DOI: https://doi.org/10.57233/ihcfs.048

ISBN: 978-978-68-07775

BOOK OF PROCEEDINGS

IHCFS – 2025 WEBSITE: fos.fugusau.edu.ng

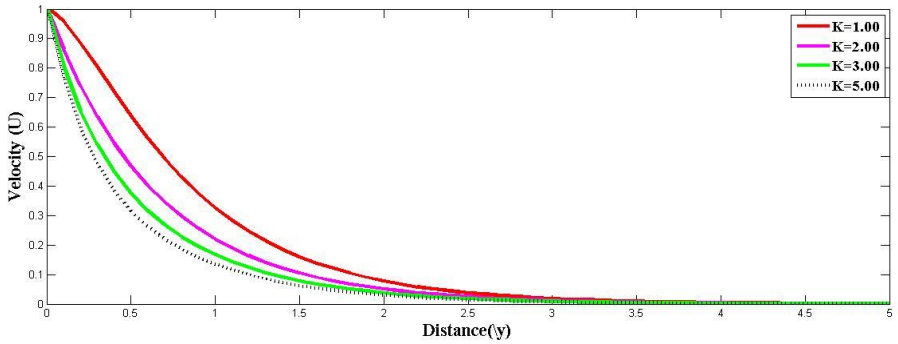

Figure 4: Velocity profile for different values of M.

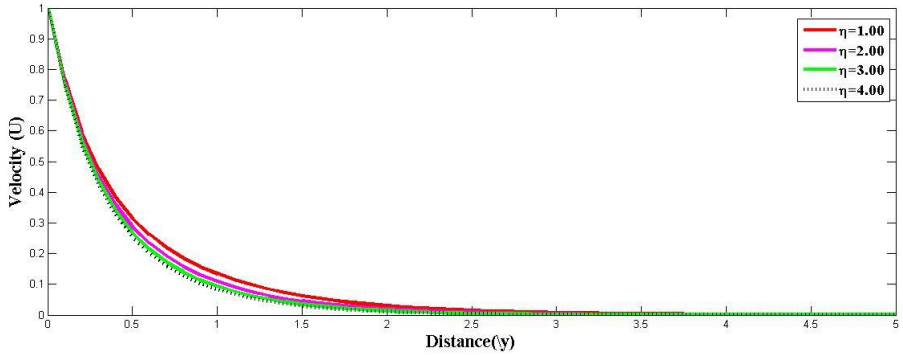

Figure 5: Velocity profile for different values of η.

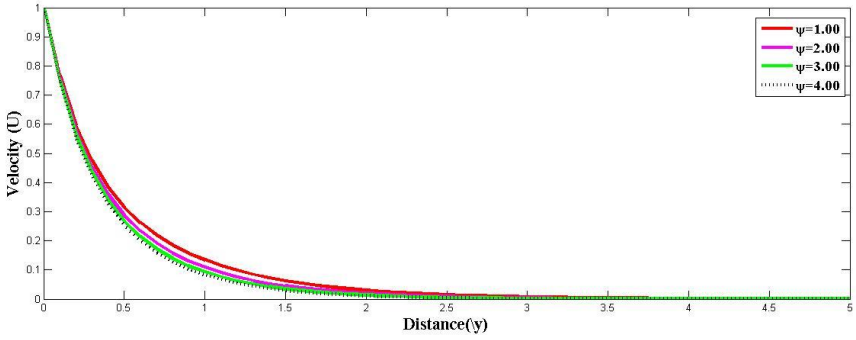

Figure 6: Velocity profile for different values of ψ.

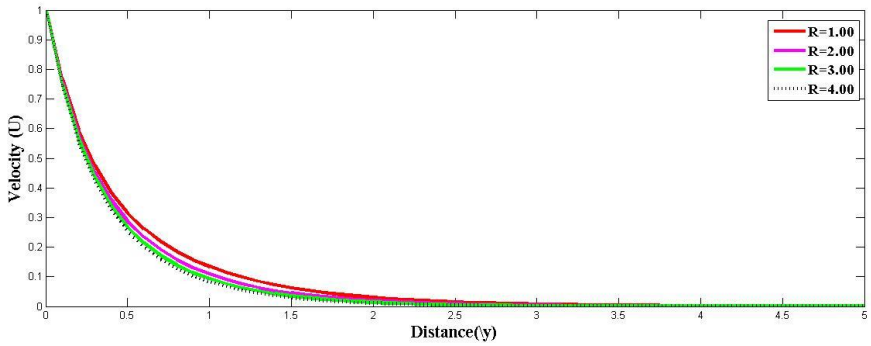

Figure 7: Velocity profile for different values of R.

DOI: https://doi.org/10.57233/ihcfs.048

ISBN: 978-978-68-07775

BOOK OF PROCEEDINGS

IHCFS – 2025 WEBSITE: fos.fugusau.edu.ng

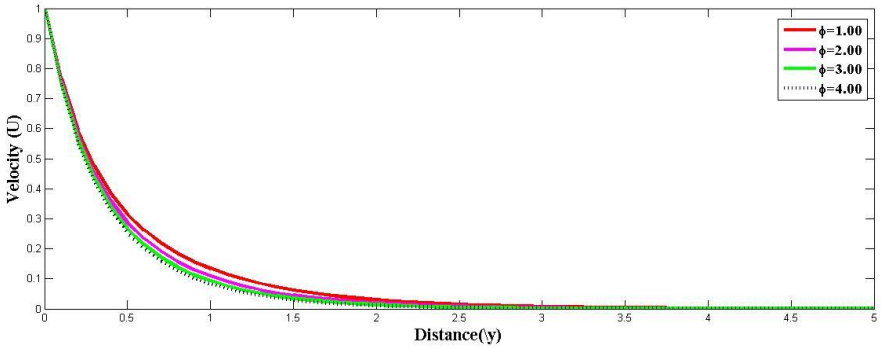

Figure 8: Velocity profile for different values of ϕ

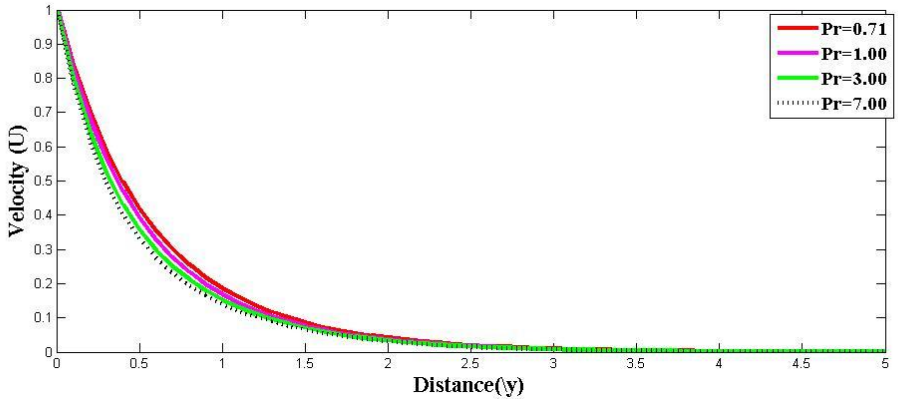

Figure 9: Velocity profile for different values of Pr

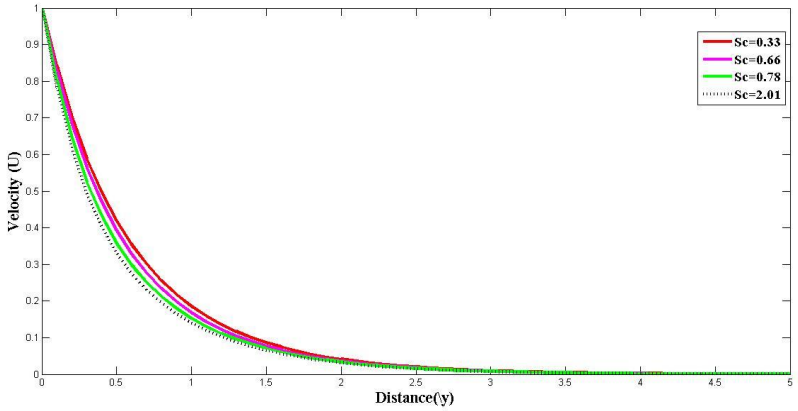

Figure 10: Velocity profile for different values of Sc.

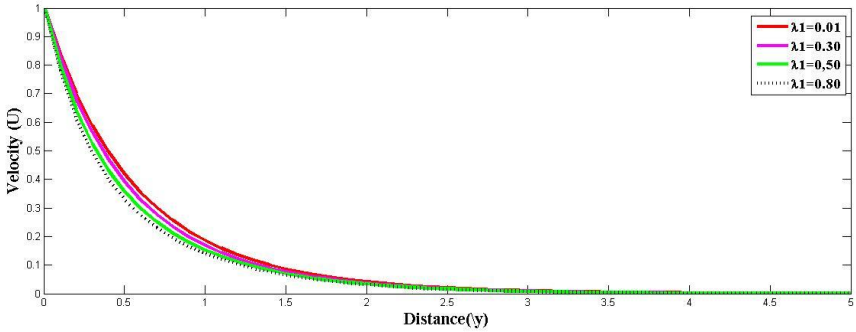

Figure 11: Velocity profile for different values of $\lambda 1$

DOI: https://doi.org/10.57233/ihcfs.048

ISBN: 978-978-68-07775

BOOK OF PROCEEDINGS

IHCFS – 2025 WEBSITE: fos.fugusau.edu.ng

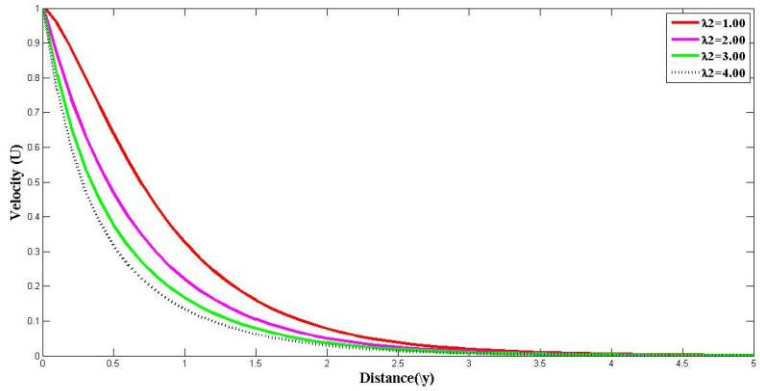

Figure 12: Velocity profile for different values of $\lambda 2$

4.2 Temperature profile

Figure 13 represents the impact of Prandtl number Pr on the temperature profiles. It is found that decrease in Prandtl number causes an increase in the thermal boundary layer of the fluid. The influence of the Dimensional concentration of the fluid on the temperature field is displayed in Figure 14. Because the heating capacity of the fluid reduces with decrease in ψ, causing the boundary of the thermally layer to be thinner. It is obvious that decrease in Prandtl value will increase the temperature of the fluid. Figure 15 displays velocity profiles for different values of η. It is seen that the momentum boundary layer decreases as ϕ become significant. With increase in η, i.e. when more radiative heat is introduced, the area around the boundary region gets far warmer. This is the case since the radiation directly introduces thermal energy into the fluid, increasing its temperature within the boundary layer

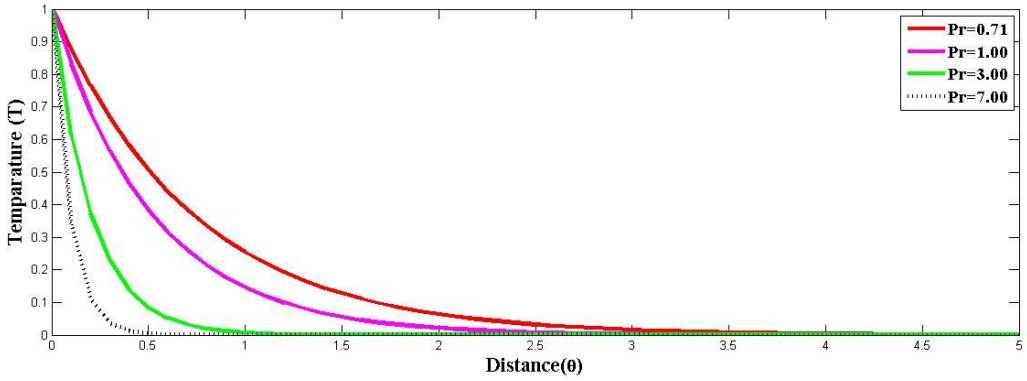

Figure 13: Velocity profile for different values of Pr

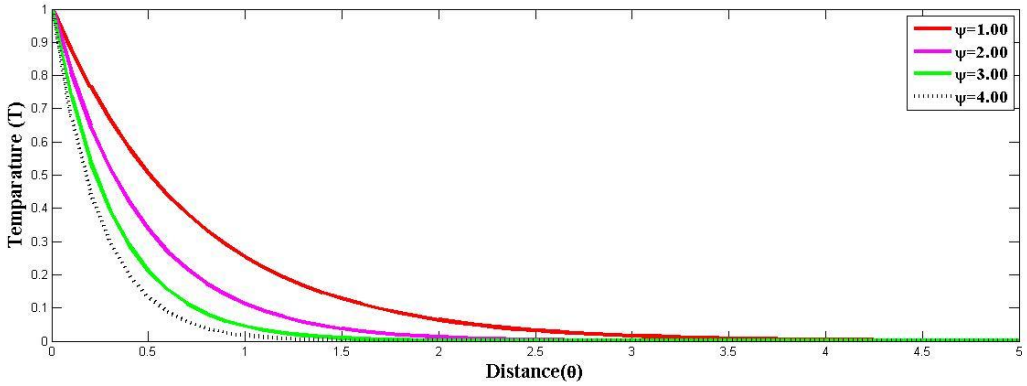

Figure 14: Velocity profile for different values of ψ

DOI: https://doi.org/10.57233/ihcfs.048

ISBN: 978-978-68-07775

BOOK OF PROCEEDINGS

IHCFS – 2025 WEBSITE: fos.fugusau.edu.ng

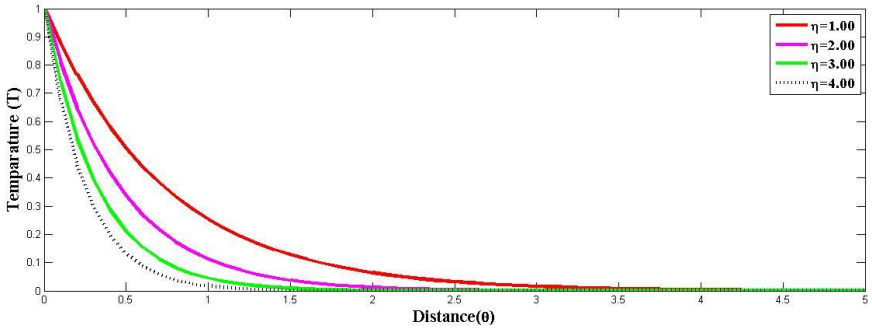

Figure 15: Velocity profile for different values of η

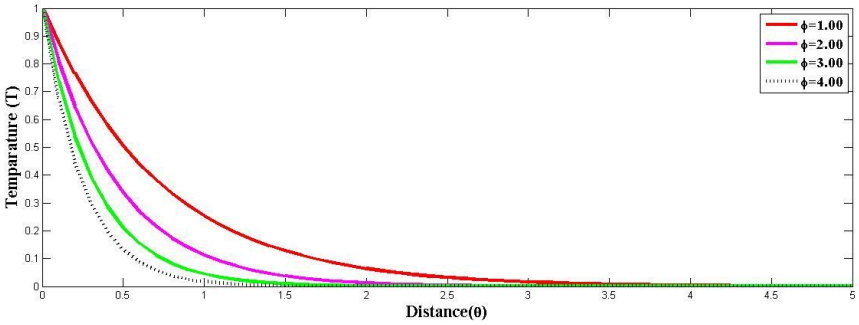

Figure 16: Velocity profile for different values of ϕ

4.3 Concentration profile

Figure 17 depicts the effect of Jeffrey parameter on the concentration profiles. It is seen that the concentration of the fluid becomes lower as Jeffrey parameter becomes significant. The concentration profiles of Figure 18 demonstrate the concentration profiles at some Schmidt values. The concentration decreases with increase in Schmidt value (Sc). The causes a narrower concentration boundary layer and reduced penetration of a solute in the fluid. Because the steeper concentration gradients are associated with slower diffusion of mass with increasing Sc. This causes a narrower concentration boundary layer and reduced penetration of a solute in the fluid. Figure 19 shows the plot of the concentration profiles for different values of Casson parameter. It is seen that the mass boundary layer decreases as η is decreased. Soret effect or thermal diffusion refers to mass flow developed because of differences in temperature. The Soret effect accelerates the mass transfer between the fluid through the fluid space, hence, making the fluid to have a lowered concentration.

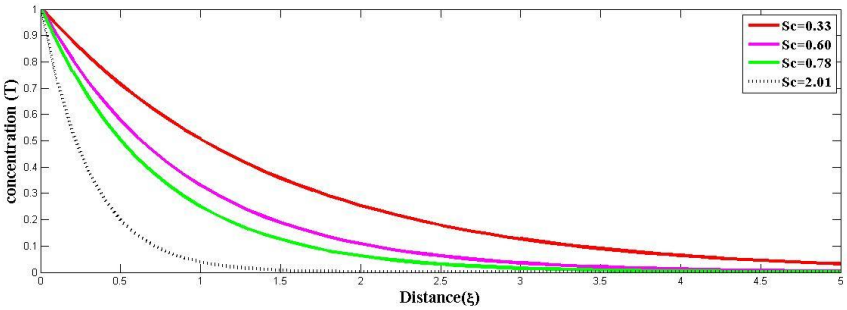

Figure 17: Velocity profile for different values of Sc

DOI: https://doi.org/10.57233/ihcfs.048

ISBN: 978-978-68-07775

BOOK OF PROCEEDINGS

IHCFS – 2025 WEBSITE: fos.fugusau.edu.ng

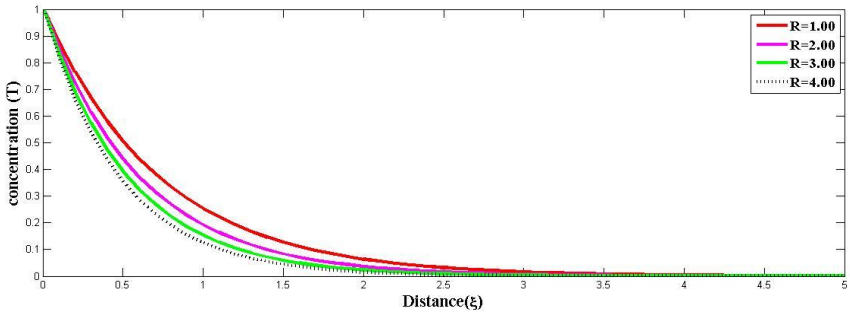

Figure 18: Velocity profile for different values of R

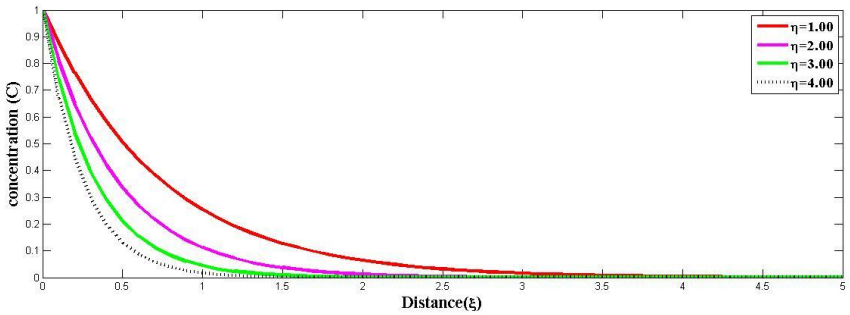

Figure 19: Velocity profile for different values of η

5.0 CONCLUSION

The present study gives the analytical solution of velocity slip effect on variable pressure and injection effects on Jefferey fluid flow in a porous medium with velocity slip condition. Specifically, the governing boundary layer equations are made up with suitable boundary conditions. The boundary layer equations are simplified and non-dimensionalized. The velocity, temperature and concentration have also been expressed which was achieved by regular perturbation method. The influence of the relevant parameters on the velocity, temperature and concentration profiles are illustrated graphically. The most significant conclusion are as follows:

i. It is observed that increasing Grashof number and slip parameter has enhancing effect on velocity.
ii. It observed that the velocity decreases with increasing Hartmann number, heat source and Jeffrey fluid parameter.
iii. It is observed intensification of slip parameter, Jeffrey fluid parameter and heat source parameter has diminishing effect on skin friction.
iv. It is observed that skin friction increases within creasing injection parameter while decreases with increasing suction parameter.

REFERENCES

Goud B. S., Srilatha P., Mahendar D., Srinivasulu T. and Reddy Y. D. (2023). Therma l radiation effect on thermostatically stratified MHD fluid flow through an accelerated vertical porous plate with viscous dissipation, *Partial Differential Equation in Applied Mathematics,* 7, 100488.

Gulle, N., and Kodi, R. (2022). Soret radiation and chemical reaction effect on MHD Jeffrey fluid flow past an inclined vertical plate embedded in porous medium. *Materials Today: Proceedings*, *50*, 2218-2226. https://dx. doi.org/10.1016/j.matpr.2021.09

Gireesha, B. J. Sowmya, G. Khan, M. I and Öztop, H. F. (2020). Flow of hybrid nanofluid across a permeable longitudinal moving fin along with thermal radiation and natural convection, *Computer Method and Programs in Biomedicine,* 185, https://dx. doi.org/105166–105166.

Hamza, M. M., Bello, I., Mustapha, A., Usman, U. and Ojemeri, G. (2023). Determining the role of thermal radiation on hydro-magnetic flow in a vertical porous super-hydrophobic microchannel, *Dutse Journal of Pure and Applied Sciences*, 9(2b), 297-308

Haritha, A., Vishali, B. and Venkata Lakshmi, C. (2022). Heat and mass transfer of MHD Jeffery nanofluid flow through a porous medium past an inclined plate with chemical reaction, radiation and soret effects. Heat Transfer. https://dx.doi.org/10.1002/htj.22735

Jamaludin A., Naganthran K., Nazar R., Pop I. (2020). Thermal radiation and MHD effect in the convection flow of Fe3 O4 water Ferrofluid towards a nonlinear moving surface, *Processes,* 8, (95). https://dx.doi.org.10.3390/pr8010095.

Naz, S., & Tamizharasi, R. (2025). Presenting a rheological model for magnetohydrodynamic Jeffrey fluid flow past an inclined permeable vertical surface under the influence of injection/suction, mixed convection and a decaying pressure gradient. *Numerical Heat Transfer, Part B: Fundamentals*, 1-22. https://doi.org/10.1080/10407790.2025.2530677

Ojemeri G., Omokhuale E., Hamza M. M., Onwubuya I. O. and Shuaibu A. (2023). A Computational Analysis on Steady MHD Casson Fluid Flow Across a Vertical Porous Channel Affected by Thermal Radiation Effect, *International Journal of Science for Global Sustainability,* 9(1).https://dx.//doi.org/10.57233/ijsgs.v9i1.393

Ojemeri, G. and Onwubuya, I. O. (2023). Analysis of mixed convection flow on arrhenius-controlled heat generating/absorbing fluid in a superhydrophobic microchannel: A semi-Analytical Approach, Dutse. *Journal of Pure and Applied Sciences.* 9, 344-357. https://doi.org/104314/dujopas.v9i2a.34.

Ojemeri, G., Onwubuya I. O., Omokhuale, E., Hussaini A. and Shuaibu, A. (2024). Analytical investigation of arrhenius kinetics with heat source/sink impacts along a heated superhydrophobic microchannel. *UMYU Scientifica,* 3(1), 61-71. DOI: https://doi.org/105619/usci.2431.004.

Omokhuale, E., & Dange, M. S. (2023a). Heat absorption effect on magnetohydrodynamic (MHD) flow of Jeffery fluid in an infinite vertical plate. *FUDMA Journal of Sciences*, 7(2), 45-51. https://doi.org/10.33003/fjs-2023-0702-1200

Omokhuale, E., & Dange, M. S. (2023b). Radiation Absorption and Chemical Reaction Effects on Magnetohydrodynamic (MHD) Flow of Jeffery Fluid in an Infinite Vertical Plate. *Journal of Pure and Applied Sciences (Science Forum*), 23(1), 417-428.

Omowaye, A.J. Fagbade, A.I. Ajayi, A.O. (2015). Dufour and Soret effects on steady MHD convective flow of a fluid in a porous medium with temperature dependent viscosity: Homotopy analysis approach. *Journal of the Nigerian Mathematical Society*, 34, 343 – 360. Doi.org/10.1016/j. jnnms.2015.08.001

Patel, H. R. (2025). Soret and heat generation effects on unsteady MHD Casson fluid flow in porous medium. *Waves in Random and Complex Media*, *35*(1), 1172-1195. https://doi.org/10.1080/17455030.2022.2030500

Rajakumar, K. V.B., Pavan Kumar, V. S. R., Balamurugan, K. S. and Bharat, V. K. (2020). Unsteady MHD Casson dissipative fluid flow past a semi-infinite vertical porous plate with radiation absorption and chemical reaction in presence of heat generation. *Journal of Mathematical Modelling of Engineering Problems.* 7(1), 160172. https://doi.org/10.18280/mmep.070120.

Raju, R. S., Reddy, G. J., Raoc, J. A. and Rashidi, M. M. (2016). Thermal diffusion and diffusion thermo effects on an unsteady heat and mass transfer magnetohydrodynamic natural convection couette flow using FEM. *Journal of Computational Design and Engineering*.3, 349–362. https://dx.doi.org/10.1016/j.jcde.2016.06.003

Sharma T., Sharma P. and Kumar N. (2022). Study of dissipative MHD oscillatory unsteady free convective flow in a vertical channel occupied with the porous material in the presence heat source effect and thermal radiation, *International Symposium on Fluids and Thermal Engineering*, 012012. https://dx.doi:10.1088/1742-6596/2178/1/012012.

Shah S. A. G.A., Hassan A. Karamti H., Alhushaybari A., Eldin S. M. and Galal A. M. (2023). Effect of thermal radiation on convective heat transfer in MHD boundary layer Carreau

Fluidwithchemicalreaction,*ScientificReports*,13,4117 .https://dx./doi.org/10.1038/s41598-023-31151-4

Vaidya, H., Rajashekhar, C., Divya, B. B., Manjunatha, G., Prasad, K. V. and Animasaun, I. L. (2020). Influence of transport properties on the peristaltic MHD Jeffrey fluid flow through a porous asymmetric tapered channel, *Results in Physics*, 18, 103295.

Wang, J., Khan, M. I., Khan, W. A., Abbas, S. Z. and Khan, M. I. (2019Transportation of heat generation/absorption and radiative heat flux in homogeneous-heterogeneous catalytic reactions of non-Newtonian fluid (Oldroyd-B model), *Computational Methods in Programs and Biomedicals*, 105310.

Zhao T., Khan M. and Chu Y. (2020) Artificial neural networking (ANN) analysis for heat and entropy generation in flow of non-Newtonian fluid between two rotating disks, Math. Method Applied Sci, https://doi.org/10.1002/mma.7310

Appendix

$$m_1 = \sqrt{\frac{(\eta Sc)^2+4(RSc)}{4}},\ m_2 = \sqrt{\frac{(\eta Sc)^2+4(R+in)Sc}{4}}, n_1 = \frac{\eta Sc}{2} + n_1,\ f_4 = \frac{-\eta Sc}{2} + n_2,$$

$$A_3 = 1,\ A_5 = \frac{\eta n_2}{n_2^2 - n_2 - (R+in)},\ A_4 = 1\text{- } A_5\ m_3 = \sqrt{\frac{(\eta pr)^2+4(\psi pr)}{4}},\ m_4 = \sqrt{\frac{(\eta pr)^2+4(\psi - in)pr}{4}}$$

$$n_5 = \frac{-\eta pr}{2} + m_3,\ n_6 = \frac{\eta pr}{2} + m_4,\ A_7 = 1 - A_8,\ A_8 = \frac{A_2 \psi pr}{f_2^2 - f_2 + \lambda pr},\ A_9 = 1 - A_{10}$$

$$A_{11} = \frac{\eta pr A_7}{n_6^2 - n_6\eta + (\psi - in)pr},\ A_{12} = \frac{\eta pr A_8}{n_2^2 - n_6\eta + (\psi - in)pr},\ A_{13} = \frac{-\eta pr A_4}{n_4^2 - n_4\eta + (\psi - in)pr},\ A_{14} = \frac{-\eta pr A_5}{n_2^2 - n_6\eta + (\psi - in)pr},$$

$$M_5\text{=}1+\lambda,\ m_6 = \sqrt{\frac{(\eta m5)^2+4\left(m+\frac{1}{k}\right)m5}{4}},\ m_7 = \sqrt{\frac{(\eta m5)^2+4\left(m+\frac{1}{k}+in\right)m5}{4}},\ n_{10} = \frac{\eta m5}{2} + m_5,\ f_{12} = \frac{\eta m5}{2} + m_6$$

$$A_{17} = \frac{-Gcm_5}{n_2^2 - \eta m_5 - \left(M+\frac{1}{k}\right)m_5},\ A_{18} = \frac{-Gcm_5}{n_6^2 - \eta m_5 n_5 - \left(M+\frac{1}{k}\right)m_5},\ A_{19} = \frac{-Gcm_5}{n_2^2 - \eta m_{5n_6} - \left(M+\frac{1}{k}\right)m_5},$$

$$A_{22} = \frac{-Grm_5 A_5}{n_4^2 - \eta m_{5n_4} - \left(M+\frac{1}{k}+in\right)m_5},\ A_{23} = \frac{-Gcm_5}{n_2^2 - \eta m_{5n_2} - \left(M+\frac{1}{k}+in\right)m_5},\ A_{24} = \frac{-Gcm_5 A_{10}}{n_8^2 - \eta m_{5n_8} - \left(M+\frac{1}{k}+in\right)m_5},$$

$$A_{25} = \frac{-Gcm_5 A_{11}}{n_{11}^2 - \eta m_{5n_{11}} - \left(M+\frac{1}{k}+in\right)m_5},\ A_{26} = \frac{-Gcm_5 A_{12}}{n_{12}^2 - \eta m_{5n_{12}} - \left(M+\frac{1}{k}+in\right)m_5},\ A_{27} = \frac{-Gcm_5 A_{13}}{n_{13}^2 - \eta m_{5n_{13}} - \left(M+\frac{1}{k}+in\right)m_5},$$

$$A_{28} = \frac{-Gcm_5 A_{14}}{n_{14}^2 - \eta m_{5n_{14}} - \left(M+\frac{1}{k}+in\right)m_5},\ A_{29} = \frac{-Gcm_5 A_{15}}{n_9^2 - \eta m_{5n_9} - \left(M+\frac{1}{k}+in\right)m_5},\ A_{30} = \frac{-Gcm_5 A_{16}}{n_{10}^2 - \eta m_{5n_{10}} - \left(M+\frac{1}{k}+in\right)m_5},$$

$$A_{31} = \frac{-Gcm_5 A_{17}}{n_7^2 - \eta m_{5n_7} - \left(M+\frac{1}{k}+in\right)m_5},\ A_{32} = \frac{-Gcm_5 A_{10}}{n_2^2 - \eta m_{5n_2} - \left(M+\frac{1}{k}+in\right)m_5}.$$